Measurement of birefringence of low-loss, high-reflectance coating of *m*-axis sapphire

Jordan B. Camp, William Kells, Martin M. Fejer, and Eric Gustafson

The birefringence of a low-loss, high-reflectance coating applied to an 8-cm-diameter sapphire crystal grown in the *m*-axis direction has been mapped. By monitoring the transmission of a high-finesse Fabry–Perot cavity as a function of the polarization of the input light, we find an upper limit for the magnitude of the birefringence of 2.5×10^{-4} rad and an upper limit in the variation in direction of the birefringence of 10 deg. These values are sufficiently small to allow consideration of *m*-axis sapphire as a substrate material for the optics of the advanced detector at the Laser Interferometer Gravitational Wave Observatory. © 2001 Optical Society of America

OCIS codes: 230.0230, 240.0310.

1. Introduction

The search for astrophysical sources of gravitational radiation will employ long-baseline laser interferometers. These include the Laser Interferometer Gravitational Wave Observatory[1] (LIGO), the VIRGO project,[2] the TAMA300 project,[3] and the GEO600 project.[4] All of these will employ a variant of a Michelson interferometer illuminated with stabilized laser light. The light will be phase modulated at radio frequency, producing modulation sidebands about the carrier frequency that provide a phase reference for sensing small variations of the interferometer arm lengths.[5] Gravitational radiation will produce a differential length change of the arms of the Michelson interferometer, causing a signal at the output port.

In Fig. 1 we show the configuration of the LIGO detector. The light from a stabilized laser source enters the interferometer, which is comprised of an asymmetric Michelson interferometer with Fabry–Perot arm cavities. The arm cavities consist of polished input and end test masses whose coated surfaces also act as mirrors to build up the laser light resonantly. An additional mirror placed between the laser and the beam splitter increases the total light power available to the arms by forming a recycling cavity together with the beam splitter and arm cavity input mirrors.[6]

The presence of noise at the interferometer output must be held below the desired strain sensitivity. The primary noise sources defining the interferometer sensitivity are seismic noise at frequencies below 100 Hz, thermal noise between roughly 100 and 300 Hz, and photon-counting noise at frequencies greater than 300 Hz. For the initial LIGO detector, the largest contribution to thermal noise comes from the internal motion of the test masses. The amplitude of this motion between 100 and 300 Hz depends inversely on both the mechanical hardness and the speed of sound in the chosen test mass material.[7] The test masses in the initial LIGO detector are made from fused silica.

Sapphire is a natural choice to consider as a test mass material for future advanced detectors because its hardness and speed of sound are both larger than those of fused silica, leading to a lower relative internal thermal noise. (Recent investigations have suggested that sapphire thermal noise may be higher than previously anticipated.[8]) Also, the relatively high thermal conductivity of sapphire may help to lessen problems of thermal distortion that are due to absorbed laser power. In addition, other considerations such as polishability, internal scatter, and growth size appear to be within the range of LIGO optical requirements. However, a concern with use of sapphire optics is the presence of possible birefringence in the coating. Present technology allows only sapphire

J. B. Camp (jordan@ligo.caltch.edu) and William Kells are with the Laser Interferometer Gravitational Wave Observatory Project, California Institute of Technology, MS 18-34, Pasadena, California 91125-8001. M. M. Fejer and E. Gustafson are with Ginzton Laboratory, Stanford University, Stanford, California 94305.

Received 19 January 2001; revised manuscript received 10 April 2001.

0003-6935/01/223753-06$15.00/0

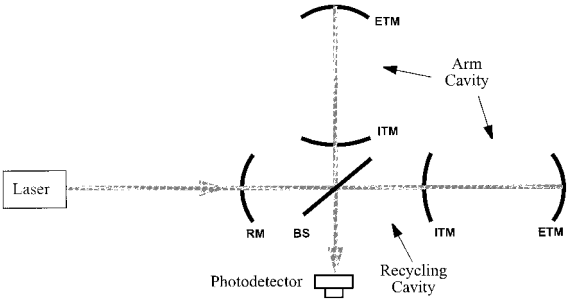

Fig. 1. Schematic diagram of the LIGO detector. ITM, input test mass; ETM, end test mass; RM, recycling mirror; BS, beam splitter.

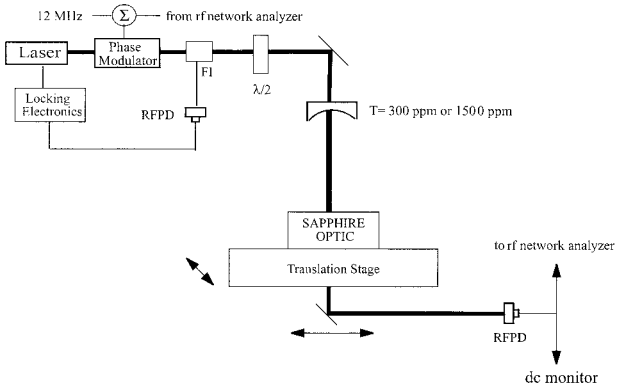

Fig. 2. Schematic diagram of apparatus. FI, Faraday isolator; λ/2, half-wave plate; RFPD, radio-frequency photodetector.

substrates grown in the *m*-axis or *a*-axis direction (both at 90 deg with respect to the uniaxial or *c*-axis direction) to be large enough for use in LIGO. The anisotropy in the thermal expansion coefficient in the surface of the *m*- or *a*-axis substrate will cause differential expansion when heated by the coating process. When the substrate cools, the corresponding, uneven contraction will stress the coating, leading to birefringence. In contrast, fused-silica optics show isotropic expansion when heated and do not cause coating birefringence.

Birefringence in the test mass coatings will affect the advanced LIGO detector in the following way. We assume that the polarization of the light incident on an arm cavity is at an angle α with respect to the optical axes of the coatings of both cavity optics. Then the light will experience a rotation of its polarization upon reflection from the arm cavity of

$$\Delta\phi = 2G_{\mathrm{arm}}\theta \sin\alpha \cos\alpha, \tag{1}$$

where G_{arm} is the optical gain of the arm cavity and θ is the coating birefringence (assumed the same for both cavity optics). This results in a fraction of power in the polarization orthogonal to the input polarization equal to $(\Delta\phi)^2$, which will be lost at the beam splitter. Given a recycling gain of G_{rc}, which we wish to preserve, the power in the orthogonal direction should be no more than of the order of $0.1/G_{\mathrm{rc}}$. For a small value of α, this leads to the condition[9]

$$\frac{0.1}{G_{\mathrm{rc}}} > 4(G_{\mathrm{arm}}\theta\alpha)^2. \tag{2}$$

For the current best estimates[10] of $G_{\mathrm{rc}} \sim 15$ and $G_{\mathrm{arm}} \sim 800$, we obtain $(\theta\alpha) < 5 \times 10^{-5}$ rad^2 as an upper limit for the allowed product of birefringence and alignment to the optical axis of the sapphire coating.

A number of experiments investigating the birefringence of low-loss mirrors have been reported. These include measurements taken at one point on the optic with a high-finesse in-vacuum Fabry–Perot cavity,[11,12] as well as a mapping of an optic in air with a one-bounce, near-normal reflection.[13] In this paper we discuss an in-air Fabry–Perot measurement that provided a map of the magnitude and direction of the birefringence of a high-reflectance coating of an 8-cm-diameter *m*-axis sapphire optic. This technique can be readily used to measure the coating birefringence of full-size LIGO optics.

2. Description of the Measurement Apparatus

The experimental setup is shown in Fig. 2. We phase modulated 100 mW of 1.06-μm laser light from a nonplanar ring oscillator at 12 MHz and also with a swept frequency from a network analyzer. It is brought through a Faraday isolator and half-wave plate and is then incident on a high-finesse Fabry–Perot cavity consisting of an input mirror with a transmission of 300 or 1500 parts per million (ppm), a radius of curvature of 1 m, and a flat coated sapphire substrate used as the output mirror. The sapphire optic is mounted on a translation stage and forms a cavity at a length of 0.35 m. The sapphire is 8 cm in diameter, 3 cm thick, with a 50-ppm transmission coating on one side and a 600-ppm reflectivity antireflection coating on the second side. The second side also has a 1-deg wedge in the *c*-axis direction. We locked the laser frequency to the cavity with the 12-MHz sideband using the Pound–Drever–Hall stabilization technique.[5] Light emerging from the cavity encounters a rf detector with a dc output to monitor the transmitted power. Not shown in Fig. 2 are a total of seven mirrors, each at an angle of 45 deg with respect to the beam, that are used to steer the beam onto the cavity. Three steering mirrors are also used to bring the light from the cavity to the detector.

The coating of the sapphire optic consisted of a quarter-wave stack of alternating SiO_2 and Ta_5O_2 layers, deposited by ion-beam sputtering.[14] The presence of birefringence in the coatings of a cavity will cause a difference in phase shift for reflected light polarized along either of the orthogonal coating optical axes. Thus the cavity resonant frequency will be split into two eigenmodes for the two polarizations. The effect of birefringence in the coatings of this cavity can then be observed experimentally in two ways. The first method involves the monitoring

of the dc light transmitted by the cavity as a function of the input light polarization. With the cavity locked to a single eigenmode, if the frequency difference between the eigenmodes is greater than the resonant width of the cavity, then only the resonant eigenmode will be transmitted by the cavity. Rotation of the light polarization will thus cause a periodic variation in the transmitted light level.

The second method is to directly observe the splitting of the cavity resonance caused by the birefringence. This can be done by use of a rf sideband that is swept through the TEM_{01} amplitude resonance of the cavity and then beats against the transmitted carrier TEM_{00} frequency at the rf detector. The frequency of this beat, which equals the frequency difference between the TEM_{00} and TEM_{01} resonances, is given by

$$(\Delta\nu_{10-00}) = \frac{c}{2\pi l}\cos^{-1}(g_1 g_2)^{1/2}, \tag{3}$$

where c is the speed of light, l is the cavity length, and $g = 1 - l/R$ is the geometric factor of the cavity mirror with radius of curvature R. For this cavity the frequency difference is ~80 MHz. To probe the resonances of both polarization eigenmodes, the input polarization is set approximately halfway between the normal modes so that both polarizations are delivered to the cavity. The laser carrier frequency for one of the modes is then locked to the cavity. As the sideband is swept, the split TEM_{01} resonances can be observed. For this method, a polarizer set at ~45-deg angle with respect to the locked carrier polarization is used to project parallel components of the sideband and carrier light onto the rf photodetector.

3. Measurements

Data were taken in two modes: with the high reflectance side of the sapphire optic on the outside of the cavity so that the resonating light passed through the substrate, and with the high reflectance side on the inside of the cavity so that the light reflected directly off the coating but did not pass through the substrate. The cavity was operated in air for all investigations.

A. Substrate in the Cavity

Data were taken in this mode to calibrate the instrument. An input mirror of 1500-ppm transmission was used. The wedge angle on the sapphire substrate gives a substrate thickness dependent on the optic transverse position, so we could tune the birefringence encountered by the light by positioning the optic:

$$\phi = (n_2 - n_1)(t + \theta_w x), \tag{4}$$

where n_2 and n_1 are the indices of refraction of the substrate fast and slow optical axes, θ_w is the wedge angle, t is the substrate thickness at the edge, and x is the location of the beam with respect to the optic edge. In Fig. 3 we show the dependence of the cavity-transmitted power with the input light polarization. The effect of the competition between the polarization eigenmodes on the locking servo made the minima in transmitted power nonrepeatable and difficult to determine to better than 20 deg. Figure 4 shows the splitting of the TEM_{01} resonance into the two eigenmodes. The peak separation depended on the optic position with a slope of ~85 kHz/μm, consistent with Eq. (4) when we assume a 1-deg wedge angle and a value of $n_2 - n_1$ for a sapphire of 0.008 rad.[15] The peak width is consistent with a cavity that has a total loss of 3200 ppm, which is due to an input mirror transmission of 1500 ppm, a loss at the antireflection surface of 2 × 600 ppm, a substrate absorption of 2 × 240 ppm,[16] and an output mirror transmission of 50 ppm.

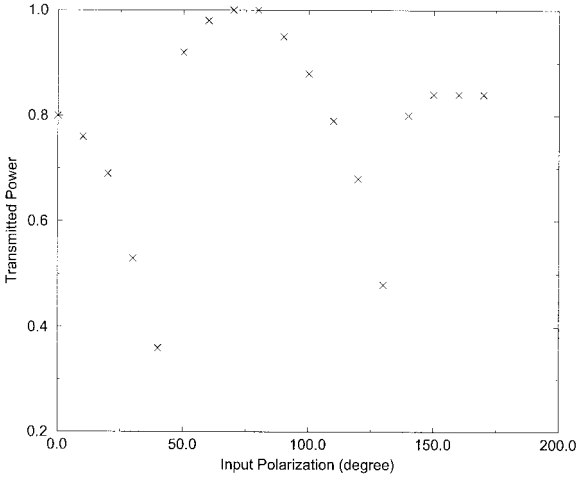

Fig. 3. Transmitted power versus input polarization of light for the substrate inside the cavity.

B. Substrate outside the Cavity

In this case the circulating light does not see the sapphire substrate, so the coating birefringence can

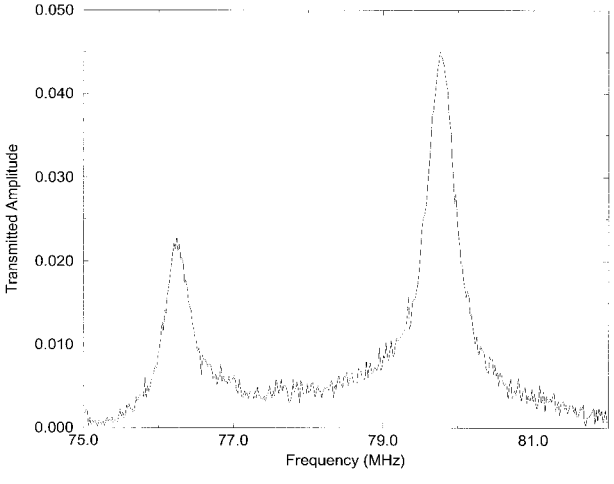

Fig. 4. Eigenfrequencies for the substrate inside the cavity. The sapphire substrate birefringence causes a splitting of the cavity TEM_{01} resonance.

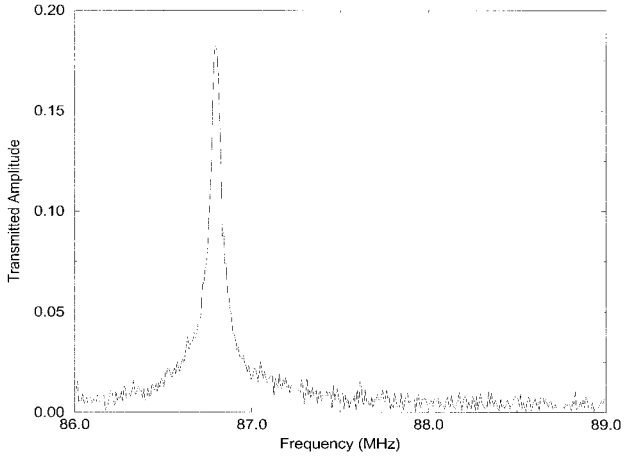

Fig. 5. Frequency spectrum for the substrate outside the cavity. The coating birefringence is too small to resolve the splitting of the TEM_{01} resonances.

be observed. To narrow the cavity linewidth, a 300-ppm transmission input mirror was used. Figure 5 shows the resonant TEM_{01} peak for this configuration, with a FWHM of 70 kHz. The splitting of this peak from the coating birefringence was not large enough to be resolved, given the width of the resonance. Data were then taken for the cavity-transmitted power dependence on polarization at nine points across the coating; noise associated with running a high-finesse cavity in air gave a 2% error in the measurement of the transmitted power. The points formed a grid centered on the optic with a point-to-point separation of ~3 cm. The point with the largest peak-to-peak variation in the transmitted intensity is shown in Fig. 6. The other points measured on the grid showed the same dependence on input polarization to within the measurement error, approximately 10 deg. We found that the angle of input polarization for which the transmitted intensity was a minimum tracked

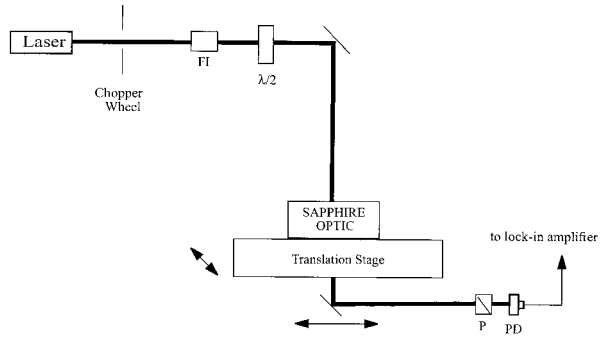

Fig. 7. Experimental setup used to determine the sapphire substrate optical axes. P, polarizer; PD, photodetector.

the rotation of the sapphire optic to within the 10-deg error.

Next we sought to compare the orientation of the coating optical axes with those of the substrate. Because of the difficulty in determining the transmission minima of Fig. 3, we did not use the measurement of Subsection 3.A to determine the substrate optical axis. Instead we examined the rotation of the polarization of the light in passing once through the sapphire substrate by removing the 300-ppm input mirror. For this measurement we used a chopper wheel and a photodetector to monitor the light transmitted by the sapphire optic (see Fig. 7). We then inserted a polarizer just before the photodetector. By adjusting the polarizer to transmit the maximum level of power at each value of the input polarization, we found the input angle that resulted in the minimum beam ellipticity in passing through the substrate. This determined the orientation of the substrate optical axes, which was found to be the same as the orientation of the coating axes to within 10 deg, as shown in Fig. 8. The crystal *c* axis was also found to be in alignment with the substrate and coating axis to within 10 deg, as shown in Figs. 6 and 8. An ad-

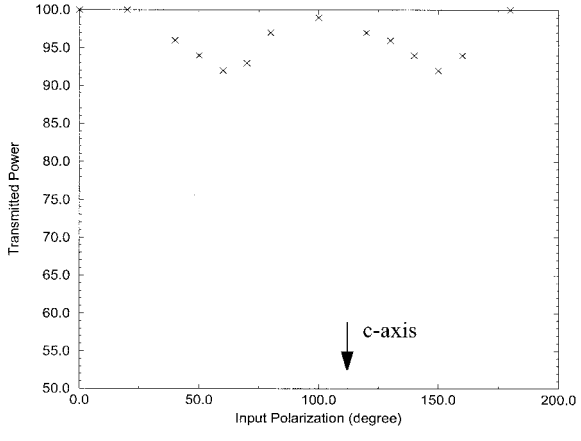

Fig. 6. Transmitted power versus input polarization for the substrate outside the cavity. The depth of the minima gives the magnitude of the coating birefringence, whereas the location of the minima gives the birefringence direction. Also shown is the orientation of the *c*-axis of the crystal.

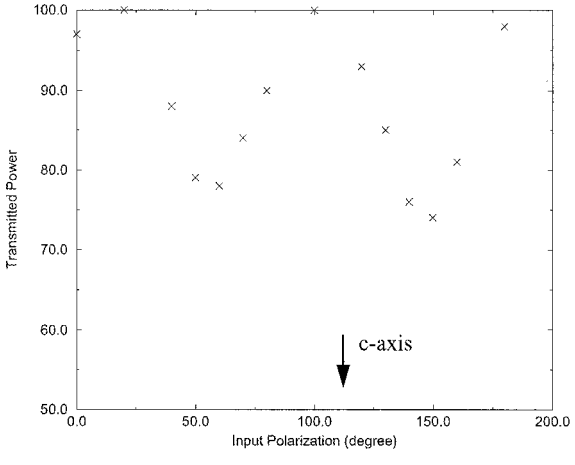

Fig. 8. Transmitted power versus input polarization for one pass through the substrate. At each point the polarizer before the detector was adjusted for maximum transmission.

ditional 5 deg of error was ascribed to the orientation of the c axis.

The relation between the transmitted power I and the difference in resonant frequency between the polarization eigenmodes $\delta\nu$ is given by

$$\frac{I}{I_0} = \cos^2(\Phi + \Phi_0) + \frac{\sin^2(\Phi + \Phi_0)}{1 + \left(\frac{\delta\nu}{\Delta\nu_{\mathrm{HWHM}}}\right)^2}, \qquad (5)$$

where I_0 is the incident power, Φ is the input polarization angle, Φ_0 is the initial offset angle of the input polarization with respect to the coating optical axes, and $\Delta\nu_{\mathrm{HWHM}}$ is the half-width of the cavity-transmitted power resonance. In Eq. (5) it is assumed that the servo is initially locked to the eigenmode represented by the first term, whereas the eigenmode of the second term is off resonance and therefore attenuated. With the resonance power half-width $\Delta\nu_{\mathrm{HWHM}}$ a factor of $\sqrt{3}$ lower than the amplitude half-width shown in Fig. 5, the 10% variation in transmitted intensity shown for the data of Fig. 6 corresponds to a resonance splitting of $\sim$10 kHz. With the relation between the cavity birefringence θ and the frequency splitting $\delta\nu$ given by

$$\theta = 2(2\pi)\frac{\delta\nu}{c}l, \qquad (6)$$

we find a coating birefringence of 1.5×10^{-4} rad. Assuming that the polarization of the cavity input light can be set to within 10 deg of the coating (and substrate) optical axes, we find an upper limit of 2.5×10^{-5} rad^2 for the quantity $(\theta\alpha)$, satisfying the requirement of inequality (2) with a factor of 2 margin.

Finally, we performed two tests with the setup of Fig. 7 to show that ellipticity in the polarization of the light induced by optics outside the resonant cavity could be neglected in our measurements. First, to test that the variations in transmitted power were due to the sapphire optic and not to the dependence of reflectivity on input polarization in the optics train somewhere between the laser and the photodetector, we removed the 300-ppm input mirror and polarizer and monitored the dc light transmitted by the sapphire optic. We found no dependence of the measured transmitted intensity on input polarization at the 1% level. For the second test, we reinserted the 300-ppm mirror and polarizer and removed the sapphire optic. By measuring the extinction ratio that could be obtained by adjusting the polarizer for each value of the input polarization, we determined that the power in the beam normal to the input polarization was less than 1%.

4. Conclusions

We have mapped the direction and magnitude of the birefringence of a low-loss, high-reflectance coating applied to an 8-cm-diameter, 3-cm-thick sapphire substrate grown in the m-axis direction. We found an upper limit for the birefringence of 2.5×10^{-4} rad and an orientation of the coating optical axes that was the same at all measured points to within 10 deg, the measurement error. We also found the coating and substrate optical axes in alignment with each other and the crystal axes to within 10 deg.

We expect these results to hold for the 32-cm-diameter, 10-cm-thick substrate size envisioned for the advanced LIGO optics for the following reasons. The coating birefringence is due to stress from differential expansion of the m-axis sapphire substrate, which is caused by heating from the coating deposition. The heat flux incident on the substrate, held initially at ambient temperature, depends on the coating deposition rate, approximately 0.1 nm/s. This rate is independent of the size of the substrate. A larger substrate will also present a larger thermal mass that will tend to limit the temperature rise. Thus we expect the same or lower birefringence for the advanced LIGO optics as the birefringence measured for the smaller optic used in this experiment. The measured values of the magnitude and direction of the birefringence give approximately a factor of 2 margin with regard to the advanced LIGO requirements, allowing use of m-axis sapphire substrates for the optics of the advanced LIGO.

An improvement to the experiment could be made by use of a lower-transmission input mirror, which would narrow the fringe width and give a steeper dependence of the transmitted power on the input polarization. This would allow the direction of the birefringence to be determined to better than the 10-deg error in this experiment. The final error would depend on the residual cavity noise, but we believe that a factor of at least 3 improvement should be possible.

We thank A. Lazzarini for his useful comments on this manuscript and P. Willems for his help in executing the experiment. This research was supported by the National Science Foundation under cooperative agreement PHY-9210038.

References

1. A. Abramovici, W. Althouse, R. W. P. Drever, Y. Gursel, S. Kawamura, F. J. Raab, D. Shoemaker, L. Sievers, R. E. Spero, R. E. Vogt, R. Weiss, S. E. Whitcomb, and M. E. Zucker, "LIGO: the Laser Interferometer Gravitational Wave Observatory," Science **256,** 325–333 (1992).
2. A. Giazotto, "The Virgo experiment: status of the art," in *First Edoardo Amaldi Conference on Gravitational Wave Experiments*, E. Coccia, G. Pizella, and F. Ronga, eds. (World Scientific, Singapore, 1995), pp. 86–99.
3. K. Tsubono, "300-m laser interferometer gravitational wave detector (TAMA300) in Japan," in *First Edoardo Amaldi Conference on Gravitational Wave Experiment*, E. Coccia, G. Pizella, and F. Ronga, eds. (World Scientific, Singapore, 1995), pp. 112–114.
4. K. Danzmann, "GEO600—a 600 m laser interferometric gravitational wave antenna," in *First Edoardo Amaldi Conference on Gravitational Wave Experiment*, E. Coccia, G. Pizella, and F. Ronga, eds. (World Scientific, Singapore, 1995), pp. 100–111.
5. R. W. P. Drever, J. L. Hall, F. V. Kowalski, J. Hough, G. M. Ford, A. J. Munley, and H. Ward, "Laser phase and frequency

stabilization using an optical resonator," Appl. Phys. B **31,** 97–105 (1983).
6. R. W. P. Drever, J. Hough, A. J. Munley, S.-A. Lee, R. Spero, S. E. Whitcomb, H. Ward, G. M. Ford, M. Hereld, N. A. Robertson, I. Kerr, J. R. Pugh, G. P. Newton, B. Meers, E. D. Brook III, and Y. Gürsel, "Gravitational wave detectors using laser interferometers and optical cavities," in *Quantum Optics, Experimental Gravity and Measurement Theory*, P. Meystre and M. O. Scully, eds. (Plenum, New York, 1983).
7. A. Gillespie and F. Raab, "Thermally excited vibrations of the mirrors of laser interferometer gravitational-wave detectors," Phys. Rev. D **52,** 577–585 (1995).
8. V. Braginsky, M. Gorodetsky, and S. Vyatchanin, "Thermodynamical fluctuations and photo-thermal shot noise in gravitational antennae," Phys. Lett. A **264,** 1–10 (1999).
9. W. Winkler, A. Rudiger, R. Schilling, K. Strain, and K. Danzmann, "Birefringence-induced losses in interferometers," Opt. Commun. **112,** 245–252 (1994).
10. K. Strain, University of Glasgow (personal communication, 2000).
11. D. Jacob, M. Vallet, F. Bretenaker, and A. Floch, "Supermirror phase anisotropy measurement," Opt. Lett. **20,** 671–673 (1995).
12. D. G. Blari, M. Notcutt, C. T. Taylor, E. K. Wong, C. Walsh, A. Leistner, J. Seckold, J.-M. Mackowski, P. Ganau, C. Michel, and L. Pinard, "Development of low-loss sapphire mirrors," Appl. Opt. **36,** 337–341 (1997).
13. P. Micossi, F. Valle, E. Milotti, E. Zavattini, C. Rizzo, and G. Ruoso, "Measurement of the birefringence properties of the reflecting surface of an interferential mirror," Appl. Phys. B **57,** 95–98 (1993).
14. The coating was provided by Research Electro-Optics, Inc., Boulder, Colo.
15. W. Driscoll, ed., *Handbook of Optics* (McGraw-Hill, New York, 1978), pp. 10–107.
16. A. Alexandrovski, Ginzton Laboratory, Stanford University, Stanford, California 94305 (personal communication, 2000).